Geophys. J. Int. (2004) **158,** 401–408 doi: 10.1111/j.1365-246X.2004.02338.x

Using commercial finite element packages for the study of earth deformations, sea levels and the state of stress

Patrick Wu

Department of Geology & Geophysics, University of Calgary, Calgary, Alberta, Canada T2N-1N4. *E-mail: ppwu@ucalgary.ca*

Accepted 2004 March 25. Received 2004 March 9; in original form 2003 October 10

SUMMARY

Modifications to commercial finite element (FE) packages must be applied before they can be used for geophysical studies involving long wavelength deformation or viscoelasticity. This paper provides in detail how and why the commercial codes have to be modified when incompressibility is assumed. Both the non-self-gravitating flat earth and self-gravitating spherical earth will be considered. The latter involves an iterative procedure, which converges within 5 iterations. This is demonstrated both analytically and numerically. In addition, implementation of the gravitationally self-consistent sea level equation on a self-gravitating spherical earth is also described. Good agreement between numerical results obtained with this coupled finite-element method and the conventional spectral method is also demonstrated. In all cases, the interpretation of the outputs of FE models are particularly important in modelling the state of stress.

Key words: finite element method, glacial rebound, mantle viscosity, sea level, stress distribution.

1 INTRODUCTION

It is well known that the finite element (FE) method is a useful technique in modelling deformation and stress in the earth: especially if the problem involves complicated geometry with large variations of material properties in arbitrary directions (e.g. Gasperini & Sabadini 1990; Wu 1991; Kaufmann *et al.* 1997, 2000) or when non-linear rheology is involved (e.g. Gasperini *et al.* 1992; Wu 1992b, 1999; Giunchi & Spada 2000; Wu 2002a,b,c). Because a number of well-tested, engineering oriented FE packages are available commercially, geoscientists are tempted to use them for the study of earth deformation and the state of stress. However, these commercial FE packages are mainly designed for engineering applications where the stiffness equation is solved. By the principle of virtual work, the stiffness equation is equivalent to the equation of motion:

$$\vec{\nabla} \cdot \overline{\overline{\tau}} = 0, \tag{1}$$

where $\overline{\overline{\tau}}$ is the stress tensor. For geophysical applications, eq. (1) is overly simplistic because it does not include the important restoring force of isostasy and self-gravitation (see eq. 3). Thus, eq. (1) is only applicable to geophysical problems involving elastic deformation with short wavelengths (p. 38 of Cathles 1975; Wu 1992a).

Although the FE technique has been used in numerous studies during the last decade, I know of no publication that discusses in detail how commercial FE packages can be modified for geophysical problems such as the post-glacial readjustment process. There are papers that mention the Wrinkler foundation (Williams & Richardson 1991) as a remedy to the restoring force of isostasy in a flat earth, but the reason behind it and the implication of its inclusion to stress studies have not been discussed. As we shall see below, the attachment of Wrinkler foundation means that the stress output from FE calculations must be modified before they can be identified with the usual physical quantity. This is an important point that may not be well understood. Furthermore, for deformations with wavelengths much larger than the diameter of the Earth, the spherical shape (Amelung & Wolf 1994) and self-gravity of the solid earth and its oceans must be included. This involves solving the gravitationally consistent sea level equation (Farrell & Clark 1976). Current development of the sea level equation is in terms of the pseudo-spectral normal mode method (Mitrovica & Peltier 1991) and the calculation of relaxation spectrum and excitation strengths of Love numbers (Wu & Peltier 1982). Because the FE approach does not calculate relaxation spectrum nor excitation strengths of Love numbers, it is not immediately clear how the sea level equation can be implemented with the FE method.

This paper discusses in detail the problem of modifying commercial FE packages for the study of deformation in a viscoelastic earth. Section 2 reviews the equations of motion and the boundary conditions used for deformation studies. In Section 3, our focus is on a non-self-gravitating, incompressible viscoelastic flat earth. The inclusion of self-gravitation in a spherical earth and its validation will be described in Section 4. Finally, the inclusion of self-gravity in the oceans and a validation of the method is also provided. Throughout the paper, the deformations are considered to be the result of glacial isostatic adjustment, but the coupled FE technique considered here can be extended to tidal, internal loading and other geophysical loading problems.

2 EQUATION OF MOTION AND BOUNDARY CONDITIONS FOR ELASTIC EARTH

In the timescale of the post-glacial adjustment process, deformation of the Earth is viscoelastic. This means that when excited by a load, the mantle initially responds like an elastic medium, but then flows like a viscous fluid over long timescales. The transition between elastic and viscous behaviour will be described by Maxwell rheology in this paper (see Wu & Peltier 1982; Martinec 2000):

$$\partial_t \overline{\overline{\tau}} = \partial_t \overline{\overline{\tau}}^0 - \frac{\mu}{\nu}(\overline{\overline{\tau}} - \Pi \overline{\overline{I}}), \tag{2a}$$

$$\overline{\overline{\tau}}^0 = \lambda\theta \overline{\overline{I}} + 2\mu\overline{\overline{\varepsilon}}, \tag{2b}$$

$$\Pi = \tfrac{1}{3}\sigma_{kk}, \tag{2c}$$

where $\overline{\overline{I}}$ is the identity matrix (with 1 along the diagonal and 0 elsewhere), $\overline{\overline{\tau}}$ and $\overline{\overline{\varepsilon}}$ are the stress and strain tensors, $\theta = \varepsilon_{kk}$ is the dilatation and λ, μ , ν are the two Lamé parameters and viscosity, respectively. For an incompressible material, $\lambda \to \infty$ but $\theta \to 0$ so that $\lambda\theta = \Pi$. In conventional methods, the Correspondence Principle (e.g. Cathles 1975; Wu & Peltier 1982) is invoked, and the problem in viscoelasticity is transformed to an associated elastic problem. For the FE method, one starts with the elastic equations of motion and boundary conditions and the stress and strain are updated from eq. (2) with some time stepping procedure (see Gasperini & Sabadini 1990; Martinec 2000, for details). Because both conventional and FE methods start with the elastic equations of motion and boundary conditions, this is where we shall begin.

For geophysical applications where the inertial force can be neglected, the linearized elastic equation of motion is typically of the form (eq. II-22 in Cathles 1975; Wu & Peltier 1982):

$$\vec{\nabla} \cdot \overline{\overline{\tau}} - \vec{\nabla}(\vec{u} \cdot \rho_o g_o \hat{r}) - \rho_1 g_o \hat{r} - \rho_o \vec{\nabla}\phi_1 = 0. \tag{3}$$

Here $\vec{u}$ is the displacement vector, $\hat{r}$ is a unit vector in the radial direction and ρ, g, ϕ are density, gravitational acceleration and gravitational potential, respectively. The subscript zero refers to the hydrostatic background state and the subscript one refers to the perturbed state. In particular, ϕ_1 contains the contribution of both the applied load and the redistribution of mass as a result of the motion of water, ice and mantle rock. The first term in eq. (3) is the divergence of stress that also appears in eq. (1). The second term represents the advection of pre-stress (Love 1911, section 154), where the hydrostatic background stress caused by the initial gravity field ($\vec{\nabla}\phi_o = g_o\hat{r}$) is carried by the material in motion. This term can be identified as the restoring force of isostasy. Although it does not appear in the viscous equation of motion (see Cathles 1975, equation II-23), it is required here so that the correct boundary condition be satisfied in the viscous limit (Wu & Peltier 1982). The importance of this term has been discussed in Wu (1992a), where it is shown that by neglecting it, there will be no viscoelastic gravitational relaxation: any mass left on the surface of the Earth will sink to the centre resulting in a singular solution at large times. The third term in eq. (3) is the result of internal buoyancy and the perturbed density is given by the linearized continuity equation:

$$\rho_1 = -\rho_0 \vec{\nabla} \cdot \vec{u} - \vec{u} \cdot (\partial_r \rho_0)\hat{r}. \tag{4}$$

In the absence of a large and negative ambient density gradient (last term in eq. 4), internal buoyancy counteracts the restoring force of isostasy (because the second and third terms in eq. 3 have comparable magnitude but opposite signs) thus instability arises (Vermeersen & Mitrovica 2000; Klemann *et al.* 2003). To avoid any instability, earth material is assumed to be incompressible here, so that internal buoyancy vanishes within homogeneous elements. One may keep the material to be compressible in eq. (2), but take internal buoyancy to be zero. In this case, instability will not arise either (Klemann *et al.* 2003), but such separation of compressibility into material part and internal buoyancy is not physically possible. Finally, the last term in eq. (3) is the result of self-gravitation, which says that the source of the gravity field is mass distribution in the Earth and any movement of earth material causes the gravity field and its potential to change according to Poisson's equation:

$$\nabla^2\phi_1 = 4\pi G\rho_1. \tag{5}$$

If internal buoyancy vanishes, then the right side of eq. (5) also vanishes and we have a Laplace equation instead.

In order to use the FE method to model the deformation of a viscoelastic earth, eq. (3) must be transformed to the same form as eq. (1). The next two sections describe such transformations for a flat earth and a spherical self-gravitating earth. Such transformations not only affect the equations of motion but also the normal stress boundary conditions as well. For completeness, the usual boundary conditions are listed below.

For an elastic earth, the boundary conditions, beside the continuity of potential $[\phi_1]_-^+ = 0$, are (Cathles 1975, p. 16–20, also Wu & Peltier 1982, eq. 48):

(i) At the surface of the Earth: $[\overline{\overline{\tau}} \cdot \hat{r}]_-^+ = 0$, so that for normal stress $\tau_{rr}|_{z=0} = -\sigma g_o$ and for shear stress $\tau_{r\theta}|_{z=0} = 0$. Here σ is the surface mass density of the applied surface load and $u_r = \vec{u} \cdot \hat{r}$. In addition, the gradient of potential satisfies $[\nabla\phi_1 \cdot \hat{r}]_-^+ + 4\pi G\rho_o u_r = 4\pi G\sigma$ at $r = a$.

(ii) At internal solid–solid boundaries, $[\overline{\overline{\tau}} \cdot \hat{r}]_-^+ = 0$, so that $\tau_{rr}|_-^+ = \tau_{r\theta}|_-^+ = 0$ at these interfaces. In addition, there is continuity of displacements $[\vec{u}]_-^+ = 0$ and $[\nabla\phi_1 \cdot \hat{r} + 4\pi G\rho_o u_r]_-^+ = 0$.

(iii) At the core–mantle boundary (CMB), $[\overline{\overline{\tau}} \cdot \hat{r}]^+ = \rho_f g_o u_r \hat{r}$. Here ρ_f is the density at the top of the fluid core and u_r is the radial displacement of the elastic–fluid boundary. Also, the shear stress vanishes at the CMB, $[\nabla\phi_1 \cdot \hat{r}]_-^+ + 4\pi G[\rho_o]_-^+ u_r = 0$ and $[\vec{u}]_-^+ = 0$. For the last condition, it should be noted that the radial displacement just above the CMB is related to the geoid change just below the CMB plus the discontinuity of the isobaric surface displacement (Chinnery 1975; Crossley & Gubbins 1975).

3 NON-SELF-GRAVITATING, INCOMPRESSIBLE FLAT EARTHS

3.1 Transformation and implementation

As discussed earlier, the aim here is to transform eq. (3) into the same form as eq. (1) for an incompressible flat earth.

Consider the equation of motion inside cells or elements where material properties (including density and elasticity) are constant (but may vary from one element to the next), then for incompressible material, the third term in eq. (3) would vanish. Furthermore, if self-gravitation were neglected, then the fourth term in eq. (3) vanishes also. Therefore, the equation of motion becomes:

$$\vec{\nabla} \cdot \overline{\overline{\tau}} - \rho_o g_o \vec{\nabla} w = 0, \tag{6}$$

where $w = \vec{u} \cdot \hat{z}$ is the vertical component of the displacement vector.

Comparing eqs (1) and (6), we see that if we define a new stress tensor (Wu & Peltier 1982, p. 438):

$$\bar{\bar{t}} = \bar{\bar{\tau}} - \rho_o g_o w \bar{\bar{I}}, \quad (7)$$

then eq. (6) can be rewritten as

$$\vec{\nabla} \cdot \bar{\bar{t}} = 0, \quad (8)$$

because

$$\vec{\nabla} \cdot \bar{\bar{t}} = \vec{\nabla} \cdot \bar{\bar{\tau}} - \rho_o g_o \vec{\nabla} w. \quad (9)$$

Note that eq. (8) is in the same form as eq. (1) except that the new stress is used. Thus, the equation of motion (eq. 6) can be recast in a form (eq. 8) suitable for the FE Method. However, as a result of the transformation (eq. 7), the boundary conditions to be applied to the FEs will be different from those listed in Section 2. In terms of the new stress components, the boundary conditions become (subscripts 1, 2 and 3 refers to x, y and the vertical direction z, respectively):

(i) $[t_{33} + \rho_o g_o w\,]_{z=0} = -\sigma g_o$ and $t_{13}]_{z=0} = 0$ on the surface of the Earth $z = 0$.

(ii) At solid–solid boundaries at depth z: $[t_{33}]_{z-}^{z+} = (\rho_- - \rho_+) g_o w$ and $t_{13}]_{z-}^{z+} = v]_{z-}^{z+} = w]_{z-}^{z+} = 0$. (Here v is the horizontal displacement.)

(iii) At solid–fluid boundary $z = -H$: $t_{13}]_{z=-H} = 0$ and $[t_{33} + \rho_s g_o w]_{z=-H} = \rho_f g_o w\,]_{z=-H}$, where the subscript s denotes the density of the solid and subscript f denotes that for the fluid. The latter condition for normal stress can be rewritten as $[t_{33}]_{z=-H} = (\rho_f - \rho_s) g_o\, [w]_{z=-H}$.

In FE models, the terms $\rho_0 g_0 w$, $(\rho_- - \rho_+) g_0 w$ or $(\rho_f - \rho_s) g_0 w$ can be simulated by Wrinkler foundation or elastic springs with spring constants $\rho_0 g_0$, $(\rho_- - \rho_+) g_0$ and $(\rho_f - \rho_s) g_0$, respectively. Because the density above the surface of the Earth can be taken as zero (for air), all the spring constants have values equal to the density contrast across the material interfaces times the vertical component of gravitational acceleration (i.e. buoyancy force). Thus, with the transformation given by eq. (7), all material interfaces of the FE model, except those with the surface normal perpendicular to the vertical, should have Wrinkler foundations attached. Where there is external (time-dependent) load applied, either on the surface of the earth for surface loading problems, or at internal boundaries for internal loading problems, one just specifies the load on those boundaries for the appropriate time step. Now the Wrinkler springs do not add any shear stress to the elements, therefore, the vanishing of the shear stress at the interfaces is satisfied automatically. This justifies the introduction of Wrinkler foundation in Williams & Richardson (1991). The implications of introducing Wrinkler foundation on stress modelling will be explored below.

3.2 Validation and stress transformation

The validity of this FE method has been demonstrated in Wu (1992b, 1993), where the results of the FE method are found to be in excellent agreement with the conventional spectral results.

For the interpretation of stress output from FE models, eq. (7) has important implications. Because the new stress tensor is used in the FE calculation, the output stress is the new stress, which must be converted back to the elastic stress through $\bar{\bar{\tau}} = \bar{\bar{t}} + \rho_o g_o w \bar{\bar{I}}$. This conversion is very important for state of stress studies. To illustrate this, the post-glacial induced normal stresses t_{33} and τ_{33} near glacial maximum in Fennoscandia are calculated with this FE method and contoured in Fig. 1. An inspection of this figure shows that, as expected, τ_{33} is the physical quantity and is mainly the result of the weight of the ice load. However, if we do not do the transformation, t_{33} is a very poor approximation of τ_{33}.

Note that the displacements are not affected by the transformation (eq. 7) and thus no conversion for displacement is necessary.

4 SPHERICAL, SELF-GRAVITATING, INCOMPRESSIBLE EARTH

4.1 The transformation for the FE method

For an incompressible spherical self-gravitating earth, eqs (3) and (5) become:

$$\vec{\nabla} \cdot \bar{\bar{\tau}} - \vec{\nabla}(\vec{u} \cdot \rho_o g_o \hat{r}) - \rho_o \vec{\nabla} \phi_1 = 0, \quad (10a)$$

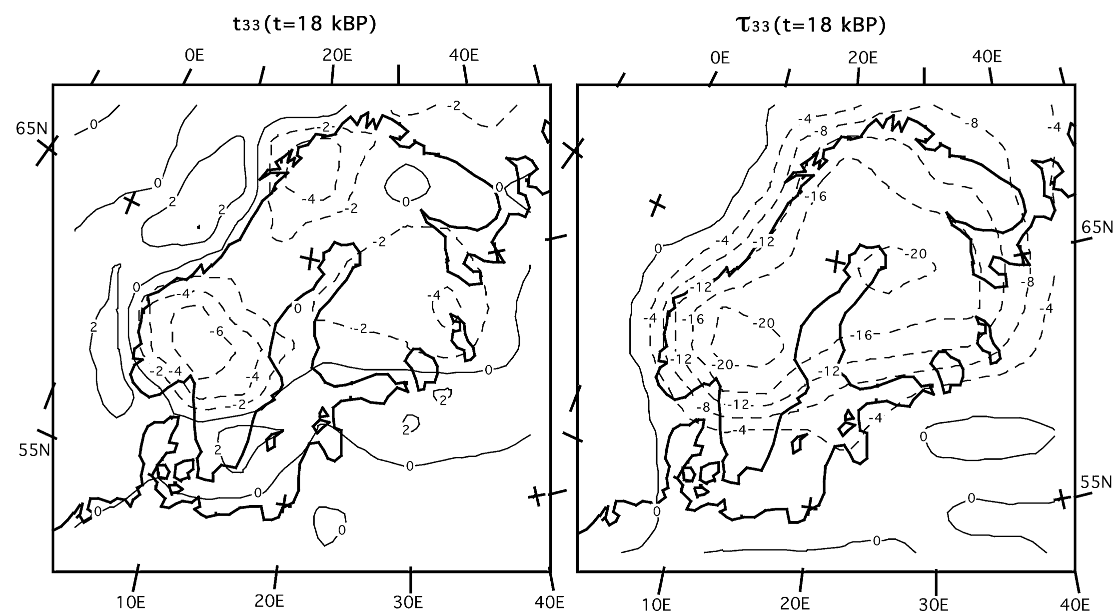

Figure 1. Contour plots of post-glacial induced normal stresses t_{33} and τ_{33} near glacial maximum in Fennoscandia. Ice load used is ICE3G (Tushingham & Peltier 1991).

$$\nabla^2 \phi_1 = 0. \tag{10b}$$

The transformation needed to make eq. (10a) into the same form as eq. (1) is (Wolf 1994):

$$\bar{\bar{t}} = \bar{\bar{\tau}} - (\rho_o g_o u_\mathrm{r} + \rho_o \phi_1)\bar{\bar{I}}, \tag{11}$$

because $\vec{\nabla} \cdot \bar{\bar{t}} = \vec{\nabla} \cdot \bar{\bar{\tau}} - \vec{\nabla}(\rho_o g_o u_\mathrm{r}) - \rho_o \vec{\nabla}\phi_1$ within elements of constant density and $u_\mathrm{r} = \vec{u} \cdot \vec{r}$. Thus, the decoupled equations to be solved for the spherical, self-gravitating incompressible earth are: $\vec{\nabla} \cdot \bar{\bar{t}} = 0$, which will be solved by the FE method, and eq. (10b), whose solution is well known. However, as we shall see below, these two equations are coupled by the normal stress boundary conditions.

(i) The surface boundary condition becomes: $[\bar{\bar{\tau}} \cdot \hat{r}]^+_- = [\{\bar{\bar{t}} + (\rho_o g_o u_\mathrm{r} + \rho_o \phi_1)\bar{\bar{I}}\} \cdot \hat{r}]^+_- = 0$. Because $[\bar{\bar{t}} \cdot \hat{r}]^+_- = -\sigma g_o - t_\mathrm{rr}$ where σ is the surface mass density of the applied load, the above condition at the surface of the Earth can be expressed as:

$$t_\mathrm{rr} + \rho_o g_o u_\mathrm{r} = -\sigma g_o - \rho_o \phi_1. \tag{12a}$$

In the FE method, the term $\rho_o\, g_o u_\mathrm{r}$ can be simulated by the Wrinkler foundation as in Section 3 and the downward load applied to the surface is now $\sigma g_o + \rho_o \phi_1$.

(ii) At internal boundaries where there is no internal mass loads, the boundary condition is $[\bar{\bar{\tau}} \cdot \hat{r}]^+_- = [t_\mathrm{rr} + \rho_o g_o u_\mathrm{r} + \rho_o \phi_1]^+_- = 0$. Because u_r, g_o and ϕ_1 are continuous across this interface and $\Delta\rho = \rho_- - \rho_+$, this therefore becomes

$$[t_\mathrm{rr}]^+_- = \Delta\rho(g_o u_\mathrm{r} + \phi_1). \tag{12b}$$

Again, in the FE method, the Wrinkler foundation and the potential load $\Delta\rho\phi_1$ must be applied at these internal boundaries.

(iii) At the CMB, $[\bar{\bar{\tau}} \cdot \hat{r}]^+ = [t_\mathrm{rr} + \rho_\mathrm{m} g_o u_\mathrm{r} + \rho_\mathrm{m}\phi_1]^+ = \rho_f g_o u_\mathrm{r} \hat{r}$, which can be rearranged to give:

$$[t_\mathrm{rr}]^+ = (\rho_f - \rho_\mathrm{m}) g_o u_\mathrm{r} - \rho_\mathrm{m}\phi_1, \tag{12c}$$

where ρ_m is the density in the mantle just above the CMB. Again, the Wrinkler foundation and the potential load $\rho_\mathrm{m}\phi_1$ must be applied at the CMB in the FE method.

All other boundary conditions for stress and displacements remain the same as those described in Section 2. If the gravitational potential ϕ_1 is known at all these interfaces, then we have the complete set of boundary conditions for the FE method.

4.2 Solution to Laplace equation

To determine the gravitational potential $\phi_1(r, \theta, \psi, t)$, the Laplace equation must be solved. Let Φ_ℓ^m be the coefficients of the spherical harmonic decomposition of $-\phi_1$ (i.e. sign is opposite to that defined in Wu & Peltier 1982), then eq. (10b) can be written as

$$\frac{\partial^2}{\partial r^2}\Phi_\ell^m + \frac{2}{r}\frac{\partial}{\partial r}\Phi_\ell^m - \frac{\ell(\ell+1)}{r^2}\Phi_\ell^m = 0. \tag{13}$$

If the density structure of the Earth is described by uniform spherical shells over a uniform sphere, then the general solution of eq. (13) inside the uniform sphere is just $\Phi_\ell^m = C_0\, r^\ell$. Within each shell, the general solution is $\Phi_\ell^m = C_1 r^\ell + C_2 r^{-(\ell+1)}$. Because the radial displacement u_r appears in the boundary condition $[\nabla\phi_1 \cdot \hat{r} + 4\pi G \rho_o u_\mathrm{r}]^+_- = 0$, knowledge of u_r is required to determine the solution to the Laplace equation. If we define the coefficient of the gradient of the potential as:

$$\Omega_\ell^m(r) = \frac{\partial}{\partial r}\Phi_\ell^m(r) + \frac{(\ell+1)}{r}\Phi_\ell^m(r), \tag{14}$$

which is related to the Farrell (1972) definition by: $Q_\ell^m(r) = \Omega_\ell^m\,(r) + 4\pi\, G\rho U_\ell^m(r)$, then the surface boundary condition becomes:

$$\Omega_\ell^m(a) = -4\pi G\big[\sigma_\ell^m + \rho_o(a) U_\ell^m(a)\big] \tag{15a}$$

and the internal boundary condition becomes:

$$\Omega_\ell^m(r^+) = \Omega_\ell^m(r^-) + 4\pi G\big[\rho_o(r^-) - \rho_o(r^+)\big] U_\ell^m(r^-) \tag{15b}$$

For simplicity, the fluid core can be treated as a uniform sphere with radius r_0. The rest of the mantle is made up of N shells with constant density. Let r_i be the outer radius of the ith shell and $\rho_i = \rho_o([r_i + r_{i-1}]/2)$ (with $r_0 < \cdots < r_i < \cdots < r_N = a$). Then using the CMB conditions described in Chinnery (1975) and Crossley & Gubbins (1975), the solution at the bottom of the mantle can be obtained. Applying the usual matrix technique to propagate the solution from one shell to the next and finally matching the boundary conditions at the surface, the coefficients $C_0, C_1, C_2, \ldots$ can be expressed in terms of the displacements at the boundaries. After some manipulation, the coefficients Φ_ℓ^m can be obtained. At the surface of the Earth $r = a$:

$$\Phi_\ell^m(a) = \frac{4\pi G}{2\ell+1} a\left[\sigma_\ell^m + \rho_o(a) U_\ell^m(a)\right] + \frac{4\pi G}{2\ell+1}\sum_{i=0}^{N-1} r_i U_\ell^m(r_i)(\rho_i - \rho_{i+1})\left(\frac{r_i}{a}\right)^{\ell+1}. \tag{16a}$$

At the CMB:

$$\Phi_\ell^m(r_o) = \frac{4\pi G}{2\ell+1} r_o\left[\sigma_\ell^m + \rho_N U_\ell^m(a)\right]\left(\frac{r_o}{a}\right)^{\ell-1} + \frac{4\pi G}{2\ell+1}\sum_{i=0}^{N-1} r_o U_\ell^m(r_i)(\rho_i - \rho_{i+1})\left(\frac{r_o}{r_i}\right)^{\ell-1} \tag{16b}$$

and at the pth interface r_p:

$$\begin{aligned}\Phi_\ell^m(r_p) = {} & \frac{4\pi G}{2\ell+1} r_p\left[\sigma_\ell^m + \rho_N U_\ell^m(a)\right]\left(\frac{r_p}{a}\right)^{\ell-1} \\ & + \frac{4\pi G}{2\ell+1}\sum_{i=p+1}^{N-1} r_p U_\ell^m(r_i)(\rho_i - \rho_{i+1})\left(\frac{r_p}{r_i}\right)^{\ell-1} \\ & + \frac{4\pi G}{2\ell+1}\sum_{i=0}^{p} r_i U_\ell^m(r_i)(\rho_i - \rho_{i+1})\left(\frac{r_i}{r_p}\right)^{\ell+1}.\end{aligned} \tag{16c}$$

Thus, given the displacements at all the interfaces, the coefficients $U_\ell^m\,(r_i)$ can be obtained and the coefficients $\Phi_\ell^m\,(r_i)$ can be calculated from eq. (16). They can be synthesized again to give $\phi_1(r_i, \theta, \psi, t)$ for the computation of the load for the FE model. This way, both the FE model and Laplace equation will be coupled together through the boundary conditions.

4.3 Coupling FE to Laplace equation

The procedure to find the deformation of a spherical, self-gravitating incompressible earth is as follows:

(i) First, the FE method is used to compute the deformation of a non-self-gravitating, spherical incompressible earth. This is achieved by taking $\phi_1 = 0$ in eq. (12) and solving $\vec{\nabla} \cdot \bar{\bar{t}} = 0$ with the FE method for all time steps (if rheology is viscoelastic).

(ii) Next, from the output of the FE method, the radial displacements $u_\mathrm{r}(r_i, \theta, \psi, t)$ and their spherical harmonic coefficients $U_\ell^m\,(r_i, t)$ at all interfaces and all time are computed.

(iii) From eq. (16), $\Phi_\ell^m(r_i, t)$ is computed and synthesized to give $\phi_1(r_i, \theta, \psi, t)$

Table 1. Iterative solution for incompressible self-gravitating uniform sphere with degree $\ell = 5$.

Iteration	U	per cent error in U	V	Φ	per cent error in Φ
0	−7.15107E-19	−30.6400	−3.90058E-20	1.04693E-17	−17.1380
1	−5.55755E-19	− 1.5287	−3.03139E-20	8.55413E-18	5.2511
2	−5.47805E-19	− 0.0763	−2.98803E-20	8.98090E-18	0.2620
3	−5.47408E-19	− 0.0038	−2.98586E-20	9.00219E-18	0.0131
4	−5.47388E-19	− 0.0002	−2.98575E-20	9.00325E-18	0.0007
5	−5.47387E-19	− 0.0000	−2.98575E-20	9.00331E-18	0.0000

(iv) Substituting $\phi_1(r_i, \theta, \psi, t)$in eq. (12) gives new loads to be applied at the interfaces in the FE model. The FE calculation is repeated with this new load.

(v) Steps 2 to 4 are repeated until the solution converges to an acceptable level. Usually it converges within 4–5 iterations.

4.4 Validation of the coupling method for a uniform sphere

To validate the procedure in the last subsection, we shall demonstrate that the coupling of the analytical solution for an incompressible, non-self-gravitating uniform sphere to Laplace solution does give the solution for an incompressible, self-gravitating uniform sphere. We shall also use the iterative procedure to see how fast the solution converges for this simple case.

The solution for an incompressible, non-self-gravitating uniform sphere is (appendix A in Wu & Ni 1996):

$$\begin{bmatrix} U \\ V \\ T_r \\ T_\theta \end{bmatrix} = \begin{bmatrix} r^{\ell+1} & r^{\ell-1} \\ \frac{(\ell+3)}{\ell(\ell+1)} r^{\ell+1} & \frac{r^{\ell-1}}{\ell} \\ 2\mu \frac{(\ell^2-\ell-3)}{\ell} r^{\ell} & 2\mu(\ell-1) r^{\ell-2} \\ 2\mu \frac{(\ell+2)}{(\ell+1)} r^{\ell} & 2\mu \frac{(\ell-1)}{\ell} r^{\ell-2} \end{bmatrix} \cdot \begin{bmatrix} C_1 \\ C_2 \end{bmatrix} \qquad (17)$$

where U, V, T_r and T_θ are the spherical harmonic coefficients for radial displacement, tangential displacement, normal and shear stress on the surface with the ℓ and m suppressed. Applying eq. (12a) and the condition of no shear stress at the surface gives:

$$U(a) = \frac{-(2\ell+1)\ell a[\sigma g - \rho\Phi(a)]}{[2\mu(\ell-1)(2\ell^2+4\ell+3) + \ell(2\ell+1)\rho g a]}, \qquad (18a)$$

$$V(a) = \frac{-3a[\sigma g - \rho\Phi(a)]}{[2\mu(\ell-1)(2\ell^2+4\ell+3) + \ell(2\ell+1)\rho g a]}. \qquad (18b)$$

For a uniform sphere, eq. (16a) gives:

$$\Phi(a) = \frac{4\pi G}{2\ell+1} a[\sigma + \rho U(a)]. \qquad (19)$$

Substituting eq. (19) into eqs (18a) and (18b), using $\sigma = \frac{2\ell+1}{4\pi a^2}$ (Longman 1962) for a point load, after some rearranging we get:

$$U(a) = \frac{-(2\ell+1)\ell\rho g a^2}{3[\mu(2\ell^2+4\ell+3) + \ell\rho g a]M_E}, \qquad (20a)$$

$$V(a) = \frac{-\rho g a^2}{[\mu(2\ell^2+4\ell+3) + \ell\rho g a]M_E}, \qquad (20b)$$

$$\Phi(a) = \frac{\mu g a(2\ell^2+4\ell+3)}{[\mu(2\ell^2+4\ell+3) + \ell\rho g a]M_E}. \qquad (20c)$$

Eqs (20a, b and c) are the solutions for an incompressible, self-gravitating uniform sphere (see eqs 33 and 12 in Wu & Peltier 1982). Thus the coupled FE method described in the last subsection is valid.

Next, we will apply the iterative procedure to the incompressible, uniform sphere and investigate how many iterations are required. The initial solution is obtained by setting $\sigma = \frac{2\ell+1}{4\pi a^2}$ and $\Phi(a) = 0$ in eq. (18) and $U(a) = 0$ in eq. (19). The first iteration is obtained by substituting the initial solution for $U(a)$ into eq. (19) and $\Phi(a)$ from the initial iteration into eq. (18). Similarly, the displacements and $\Phi(a)$ can be updated through iterations. Because the actual solution is given by eq. (20), the percentage error of the nth iteration can be computed. The results for angular order $\ell = 5$ are all listed in Table 1, from which it can be seen that the exact solution is achieved after 5 iterations. For $\ell = 2$, the exact solution is reached after 9 iterations, although at the 4th iterations, the solution is within 0.4 per cent of the actual solution and for the 5th iteration the percentage error falls below 0.1 per cent. Thus, only 4 to 5 iterations are required in general.

4.5 Validation of the coupling method for a layered earth

Next, a layered earth that consists of a uniform viscoelastic shell overlying an inviscid fluid core is considered. This model is chosen because analytical solutions for both self-gravitating and non-self-gravitating cases can be obtained by the technique described in Wu & Ni (1996). The load is a Heaviside harmonic load with degree $\ell = 2$. Fig. 2 shows that the agreement between the solution obtained using the iterative method (after 5 iterations) and the analytical method is well within 1 per cent. The FE model is axisymmetric with 360 elements from the north pole to the south and 18 layers in the mantle. Better accuracy can be achieved with finer elements and better spatial resolution, but that would put more demand on computer resources.

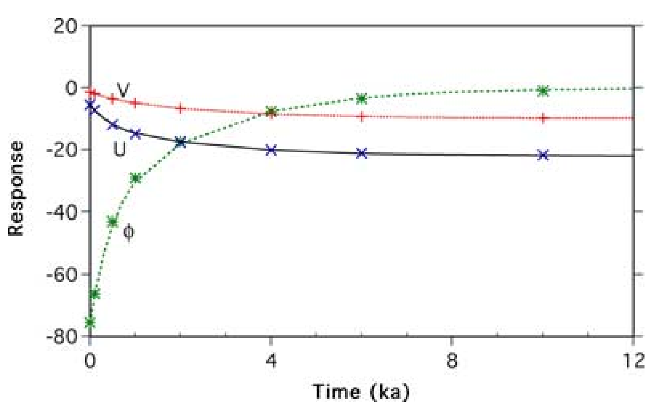

Figure 2. Comparing theoretical results (lines) to results from the Coupled FE method (symbols) for $\ell = 2$ Heaviside deformation in a self-gravitating uniform viscoelastic shell over uniform inviscid fluid core.

5 SEA LEVEL COMPUTATION WITH COUPLED FE–LAPLACE METHOD

The above section describes how the solid mantle deforms. Because the Earth is self-gravitating, all deformations perturb the gravitational field and thus the geoid. However, sea level records measure the change in the geoid ($\phi_1(a, \theta, \psi, t)/g$) relative to the solid surface of the Earth, which is displaced by $u_r(a, \theta, \psi, t) = U(\theta, \psi, t)$ in the radial direction. Excluding the effects of time-dependent ocean margin (Johnston 1993; Milne 1998; Peltier 1998), near-field water influx (Milne 1998; Peltier 1998; Milne *et al.* 1999) and earth rotation (Milne & Mitrovica 1998; Peltier 1998), the consistent sea level equation is given by (Farrell & Clark 1976; Mitrovica & Peltier 1991):

$$S(\theta, \psi, t) = \phi_1(\theta, \psi, t)/g - U(\theta, \psi, t) + c(t)]O(\theta, \psi), \tag{21}$$

where $O\theta, \psi$ is the Ocean function and $c(t)$ is a time dependent quantity required to conserve mass and is given by:

$$c(t) = -\frac{M_I(t)}{\rho_w A_o} - \frac{1}{A_o}\left\langle \frac{\phi_1}{g} - U \right\rangle_o . \tag{22}$$

Here A_o is the area of the ocean basins, ρ_w is the density of water, $M_I(t)$ is the mass loss history of the ice at time t and $\langle\,\rangle_o$ represents integration over the ocean basins. Because the terms in $\langle\,\rangle_o$ are independent of location, $c(t)$ is called the eustatic sea level and the first term on the right is the ice-equivalent sea level (Milne *et al.* 2002). Traditionally eq. (21) is also solved using the iterative (relaxation) technique, but one need not solve the coupled FE–Laplace equation first, and then the consistent sea level equation. Both can be solved simultaneously using the following procedure:

(i) Given the ice load history, one can determine the water load in the oceans by assuming that sea level is given by the ice-equivalent sea level $S_o(t) = -\frac{M_I(t)}{\rho_w A_o} O(\theta, \psi)$. As a result of the conservation of mass, the spherical harmonic degree zero component of the combined ice and water load is zero.

(ii) The combined ice and water load generally has a degree-one component that causes a rigid shift in the centre of mass (Farrell 1972; Cathles 1975). Because we are not interested in the rigid shift, it will be removed. This is achieved by decomposing the load into its spherical harmonic components and subtracting the degree-one component from the combined load to give the new surface load.

(iii) This new surface load with no degree-zero and degree-one components is now applied to a non-self-gravitating spherical earth (i.e. taking $\phi_1 = 0$ in eq. (12) and solving $\vec{\nabla} \cdot \bar{\bar{t}} = 0$ with the FE method for all time steps).

(iv) Next, from the output of the FE method, the radial displacements $u_r(r_i, \theta, \psi, t)$ and their spherical harmonic coefficients $U_\ell^m(r_i, t)$ at all interfaces and all time are computed.

(v) From eq. (16), $\Phi_\ell^m(r_i, t)$ is computed and synthesized to give $\phi_1(r_i, \theta, \psi, t)$.

(vi) Substitute the above computed $\phi_1(a, \theta, \psi, t)$ and $U(\theta, \psi, t)$ into eq. (22) to compute $c(t)$. Thus the sea level $S(\theta, \psi, t)$ for all time steps can be calculated using eq. (21).

(vii) The ice load history and the updated sea level $S(\theta, \psi, t)$ now gives the new combined ice and water load at the surface. With the degree-one component removed from the new combined ice and water load, the surface mass density σ can be computed. Together with the updated surface potential perturbation, the right side of eq. (12a) can be obtained. From the potential perturbation at the other internal boundaries or the CMB, the potential load on the right side of eqs (12b) and (12c) can also be evaluated. These are the new boundary conditions to be applied on the FE model.

(v) Steps 3 to 7 are repeated until the solution converges to an acceptable level. Again, numerical tests show that the solution converges within 5 iterations.

Validity of this new method is shown in Fig. 3 where the result of this method is compared with that computed with the pseudo-spectral method (Mitrovica & Peltier 1991). The result of this latter method is provided by Wouter van der Wal of TU Delft, who modified the pseudo-spectral sea level program coded by G. Di Donato (Di Donato *et al.* 2000) and benchmarked with J.X. Mitrovica's program. The load considered is a 15-degree uniform disc load (pressure of 24 MPa) with complementary ocean. The ice load is left on the north pole of a self-gravitating incompressible spherical earth, which consists of a 100-km thick lithosphere overlying a uniform 10^{21} Pa s viscoelastic mantle and an inviscid fluid core. For this earth and ice model, the pseudo-spectral method summed harmonic contributions up to degree 128. In the new method, Laplace's equation is solved with harmonics up to degree 180, but the load spectrum is

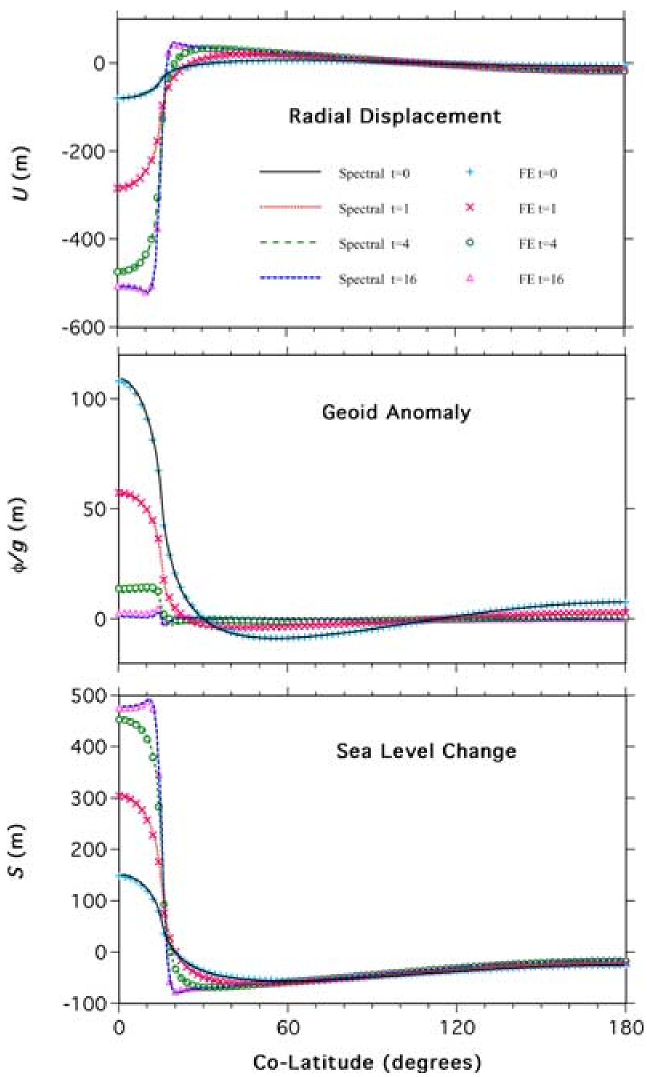

Figure 3. Evolution of the surface radial displacement, geoid anomaly and sea level change as a result of Heaviside loading of a 15-degree uniform disc load. The spherical self-gravitating earth contains a 100-km thick lithosphere overlying a uniform 10^{21} Pa s viscoelastic mantle and an inviscid fluid core. The lines are predictions of the pseudo-spectral method. These are compared to the results of the sea level equation solved with the finite element (FE) model coupled to Laplace equation (symbols).

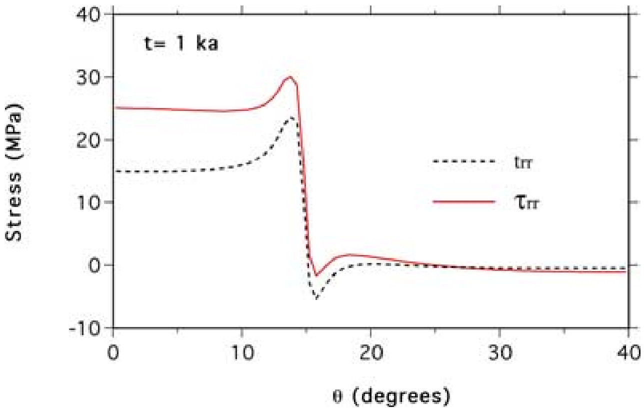

Figure 4. Plot of $t_{\rm rr}$ and $\tau_{\rm rr}$ at $t = 1$ ka after the Heaviside loading of a 15-degree uniform disc load on a 100-km thick lithosphere overlying a uniform 10^{21} Pa s viscoelastic mantle and an inviscid fluid core.

tapered with a cosine filter above degree 120 to reduce Gibb's effect at the centre. As a result of the truncation of the higher harmonics, Gibb's effect becomes severe near the edge of the sharp-corner load even after the spectrum has been tapered. This effect is especially important for the calculation of the potential perturbation or geoid anomaly, but is less severe in the radial displacement because of the presence of the elastic lithosphere.

The evolution of the surface displacement in the radial direction $U(\theta, t)$, the geoid anomaly $\phi_1(\theta, t)/g$ and the sea level change $S(\theta, t)$ are computed and plotted in Fig. 3. Although no actual sea level change occurs on land, eq. (21) is also applied over the ice to give the plot in Fig. 3. The symbols are the results of this new method, while the lines are those computed with the pseudo-spectral method. Despite their vast differences in approach, Fig. 3 shows excellent agreement between them. The difference in $S(\theta,\, t)$ is below 3 per cent except near the edge of the load where Gibb's effect becomes important.

Again, the stress output from the FE calculation has to be converted according to eq. (11):

$$\overline{\overline{\tau}} = \overline{\overline{t}} + [\rho_o g_o u_{\rm r} + \rho_o \phi_1]\overline{\overline{I}} \tag{23}$$

The importance of this conversion is shown in Fig. 4 where the normal radial stress $t_{\rm rr}$ and $\tau_{\rm rr} = t_{\rm rr} + \rho_o g_o u_{\rm r} + \rho_o \phi_1$ at $t = 1$ ka are plotted. The ice and ocean models are the same as that in Fig. 3. With the inclusion of the terms $\rho_o\, g_o u_{\rm r} + \rho_o \phi_1$, the magnitude of the normal stress is now much closer to the applied ice and ocean load. Thus, Fig. 4 shows that one cannot take the stress output of FE as the physical quantities.

6 CONCLUSIONS

This paper shows how commercial FE packages can be used to model deformations in a non-self-gravitating flat-earth or self-gravitating spherical earth. The implementation of the consistent sea level equation is also discussed.

Because commercial FE packages solve a different equation of motion, the stress transformation given by eq. (7) or (11) must be applied before they can be used to calculate the deformation or the state of stress of an incompressible earth. The application of the stress transformation means that:

(i) Boundary conditions for the FE method must be modified so that Wrinkler foundations with the spring constant equal to the density contrast across the material interfaces times the vertical (radial) component of gravitational acceleration (i.e. buoyancy force) are applied to every non-vertical material boundary.

(ii) The stress output from the FE program must be converted back to its physical quantity before it becomes useful for interpretation.

For the self-gravitating spherical earth, the usual system of equations is decoupled, so that one may solve the FE equation and Laplace equation separately. However, because the decoupled system is coupled by the boundary conditions, the coupling can be achieved via the iteration (relaxation) technique. Solving the basic sea level equation is no more complicated than that for the solid earth. It also involves the relaxation method and the solution is found to converge within 4 to 5 iterations. This iterative technique is shown to give results comparable to the conventional normal mode approach. The advantage of this method is its ease in the inclusion of lateral heterogeneity (Wu & Van der Wal 2003; Wu *et al.* 2004) and non-linear rheology. The latter is possible because mode coupling (Wu 2002c) and non-linearity (Wu 2002b) only affect the FE part of the calculation but not the solution to the Laplace equation.

ACKNOWLEDGMENTS

Special thanks to Wouter van der Wal of TU Delft, who supplied the pseudo-spectral sea level computation in Fig. 3. The author is also indebted to Dr Bert Vermeersen and Dr Hansheng Wang for their constructive comments on the manuscript. The FE calculation was performed with the ABAQUS package from Hibbitt, Karlsson and Sorensen Inc. This research is supported by an Operating Grant from NSERC of Canada.

REFERENCES

Amelung, F. & Wolf, D., 1994. Viscoelastic perturbations of the Earth: significance of the incremental gravitational force in models of glacial isostasy, *Geophys. J.,* **117,** 864–879.

Cathles, L.M., 1975. *The Viscosity of the Earth's Mantle*. Princeton University Press, Princeton, NJ.

Chinnery, M.A., 1975. The static deformation of an earth with a fluid core: a physical approach, *Geophys. J. R. astr. Soc.,* **42,** 461–475.

Crossley, D.J. & Gubbins, D., 1975. Static deformation of the Earth's liquid core, *Geophys. Res. Lett.,* **2,** 1–4.

Di Donato, G., Vermeersen, L.L.A. & Sabadini, R., 2000. Sea-level changes, geoid and graviy anomalies due to Pleistocene deglaciation by means of multilayered, analytical Earth models, *Tectonophys.,* **320,** 409–418.

Farrell, W.E., 1972. Deformations of the Earth by surface loads, *Rev. Geophys. Space Phys.,* **10,** 761–797.

Farrell, W.E. & Clark, J.A., 1976. On postglacial sea level, *Geophys. J. R. astr. Soc.,* **46,** 647–667.

Gasperini, P. & Sabadini, R., 1990. Finite element modeling of lateral viscosity heterogeneities and post-glacial rebound, *Tectonophysics,* **179,** 141–149.

Gasperini, P., Yuen, D.A. & Sabadini, R., 1992. Postglacial rebound with a non-Newtonian upper mantle and a Newtonian lower mantle rheology, *Geophys. Res. Lett.,* **19,** 1711–1714.

Giunchi, C. & Spada, G., 2000. Postglacial rebound in a non-Newtonian spherical Earth, *Geophys. Res. Lett.,* **27,** 2065–2068.

Johnston, P., 1993. The effect of spatially non-uniform water loads on predictions of sea-level change, *Geophys. J. Int.,* **114,** 615–634.

Kaufmann, G., Wu, P. & Wolf, D., 1997. Some effects of lateral heterogeneities in the upper mantle on postglacial land uplift close to continental margins, *Geophys. J. Int.,* **128,** 175–187.

Kaufmann, G., Wu, P. & Li, G., 2000. Glacial isostatic adjustment in Fennoscandia for a laterally heterogeneous earth, *Geophys. J. Int.,* **143,** 262–273.

Klemann, V., Wu, P. & Wolf, D., 2003. Compressible viscoelasticity: stability of solutions for homogeneous plane earth models, *Geophys. J. Int.,* **153,** 569–585.

Longman, I.M., 1962. A Green's Function for determining the deformation of the Earth under surface mass loads 1. Theory, *J. geophys. Res.,* **67**(2), 845–950.

Love, A.E.H., 1911. *Some Problems of Geodynamics,* Dover, New York.

Martinec, Z., 2000. Spectral-finite element approach to three-dimensional viscoelastic relaxation in a spherical earth, *Geophys. J. Int.,* **142,** 117–141.

Milne, G.A., 1998. Refining models of the glacial isostatic adjustment process, *PhD thesis*, University of Toronto, Toronto, p. 124

Milne, G.A. & Mitrovica, J.X., 1998. Postglacial sealevel change on a rotating Earth, *Geophys. J. Int.,* **133,** 1–19.

Milne, G.A., Mitrovica, J.X. & Davis, J.L., 1999. Near-field hydro-isostasy: the implementation of a revised sea-level equation, *Geophys. J. Int.,* **139,** 464–482.

Milne, G.A., Mitrovica, J.X. & Schrag, D.P., 2002. Estimating past continental ice volume from sea-level data, *Quat. Sci. Rev.,* **21,** 361–376.

Mitrovica, J.X. & Peltier, W.R., 1991. On postglacial geoid subsidence over the equatorial oceans, *J. Geophys. Res.,* **96,** 20 053–20 071.

Peltier, W.R., 1998. Postglacial variations in the level of the sea: implications for climate dynamics and solid-earth geophysics, *Rev. Geophys.,* **36,** 603–689.

Tushingham, A.M. & Peltier, W.R., 1991. Ice-3G: a new global model of late Pleistocene deglaciation based upon geophysical predictions of post-glacial relative sea-level change, *J. geophys. Res.,* **96,** 4497–4523.

Vermeersen, L.L.A. & Mitrovica, J.X., 2000. Gravitational stability of spherical self-gravitating relaxation models, *Geophys. J. Int.,* **142,** 351–360.

Williams, C.A. & Richardson, R.M., 1991. A rheologically layered three-dimensional model of San Andreas fault in central and southern California, *J. geophys. Res.,* **96,** 16 597–16 623.

Wolf, D., 1994. Lamé's problem of gravitational viscoelasticity: the isochemical, incompressible planet, *Geophys. J. Int.,* **116,** 321–348.

Wu, P., 1991. Flexure of Lithosphere beneath the Alberta Foreland Basin: Evidence of an eastward stiffening continental lithosphere, *Geophys. Res. Lett.,* **18,** 451–454.

Wu, P., 1992a. Viscoelastic vs. Viscous deformation and the advection of prestress, *Geophys. J. Int.,* **108,** 35–51.

Wu, P., 1992b. Deformation of an incompressible viscoelastic flat earth with Power Law Creep: a Finite Element approach, *Geophys. J. Int.,* **108,** 136–142.

Wu, P., 1993. Post-glacial Rebound in a Power-law medium with Axial symmetry and the existence of the Transition zone in Relative Sea Level data, *Geophys. J. Int.,* **114,** 417–432.

Wu, P., 1999. Modeling Postglacial Sea-Levels with Power Law Rheology and Realistic Ice Model in the Absence of Ambient Tectonic Stress, *Geophys. J. Int.,* **139,** 691–702.

Wu, P., 2002a. Effects of Stress Exponent in Mantle Flow Law on Postglacial Induced Surface Motion and Gravity in Laurentia, *Geophys. J. Int.,* **148,** 676–686.

Wu, P., 2002b. Effects of nonlinear rheology on degree 2 harmonic deformation in a spherical self-gravitating earth, *Geophys. Res. Lett.,* **29**(8), 10.1029/2001GL014109.

Wu, P., 2002. Mode coupling in a viscoelastic self-gravitating spherical earth induced by axisymmetric loads and lateral viscosity variations, *Earth planet. Sci. Lett.,* **202,** 49–60.

Wu, P. & Peltier, W.R., 1982. Viscous gravitational relaxation, *Geophys. J. R. astr. Soc.,* **70,** 435–486.

Wu, P. & Ni, Z., 1996. Some analytical solutions for the viscoelastic gravitational relaxation of a two-layer non-self-gravitating incompressible spherical earth, *Geophys. J. Int.,* **126,** 413–436.

Wu, P. & Van der Wal, W., 2003. Postglacial sea-levels on a spherical, self-gravitating viscoelastic earth: effects of lateral viscosity variations in the upper mantle on the inference of viscosity contrasts in the lower mantle, *Earth and Planet. Sci. Lett.,* **211,** 57–68.

Wu, P., Wang, H.S. & Schotman, H., 2004. Postglacial induced surface motions, sea-levels & geoid rates on a spherical, self-gravitating, laterally heterogeneous Earth, *Journal of Geodynamics,* in press.